A centrifuge method to determine the solid–liquid phase behavior of eutectic mixtures

A centrifuge method to determine the solid–liquid phase behavior of eutectic mixtures

Adriaan van den Bruinhorst, Laura J. B. M. Kollau, Maaike C. Kroon, Jan Meuldijk, Remco Tuinier, and A. Catarina C. Esteves

Citation: J. Chem. Phys. **149**, 224505 (2018); doi: 10.1063/1.5051515
View online: https://doi.org/10.1063/1.5051515
View Table of Contents: http://aip.scitation.org/toc/jcp/149/22
Published by the American Institute of Physics

A centrifuge method to determine the solid–liquid phase behavior of eutectic mixtures

Adriaan van den Bruinhorst,[1,2,a)] Laura J. B. M. Kollau,[1] Maaike C. Kroon,[2,b)] Jan Meuldijk,[3] Remco Tuinier,[1] and A. Catarina C. Esteves[1,a)]
[1]*Laboratory of Physical Chemistry, Department of Chemical Engineering and Chemistry, Eindhoven University of Technology, Het Kranenveld, Building 14 (Helix), 5612 AZ Eindhoven, The Netherlands*
[2]*Separation Technology Group, Department of Chemical Engineering and Chemistry, Eindhoven University of Technology, Het Kranenveld, Building 14 (Helix), 5612 AZ Eindhoven, The Netherlands*
[3]*Laboratory of Chemical Reactor Engineering/Polymer Reaction Engineering, Department of Chemical Engineering and Chemistry, Eindhoven University of Technology, Het Kranenveld, Building 14 (Helix), 5612 AZ Eindhoven, The Netherlands*

(Received 9 August 2018; accepted 24 November 2018; published online 11 December 2018)

The centrifuge method is a novel, equilibrium-based, analytical procedure that allows the construction of solid–liquid phase diagrams of binary eutectic mixtures. In this paper, the development, optimization, and successful verification of the centrifuge method are described. Contrary to common dynamic analysis techniques—differential scanning calorimetry and hot-stage microscopy—the studied mixtures are equilibrated at constant temperature. Therefore, the mixtures do not need to be recrystallized from the melt during analysis. This offers a great advantage for mixtures that exhibit strong supercooling behavior rather than direct crystallization. The centrifuge method was verified by reproducing the binary eutectic phase behavior of both the nearly ideal biphenyl–bibenzyl system and the strongly non-ideal deep eutectic solvent (DES) urea–choline chloride, which is prone to supercooling. Hence, the centrifuge method offers an alternative route to common dynamic analysis techniques for the quantification of the liquid range of DESs and other binary eutectic mixtures. *Published by AIP Publishing.* https://doi.org/10.1063/1.5051515

I. INTRODUCTION

Since the introduction of the term deep eutectic solvents (DESs) in 2003,[1] studies directed at the application of molten eutectic mixtures as liquid media have emerged tremendously. A eutectic mixture can result from mixing two (or more) components, yielding liquids at temperatures below the melting temperature of their pure constituents.[2] Any binary mixture with immiscibility in the solid phase and miscibility in the liquid phase shows eutectic behavior.[2] The physicochemical properties of liquid eutectic mixtures depend on their constituents and can be further tuned by changing the composition of the mixture. Hence, eutectic mixtures have been investigated for a wide variety of applications, e.g., electrochemistry,[3] polymerization,[4] thermal energy storage,[5,6] pharmaceuticals,[7,8] and liquid–liquid extraction.[9,10]

Whether a eutectic mixture can be applied as a stable liquid is determined by its phase behavior. At a certain operating temperature (and pressure), the liquid range of a simple eutectic mixture is confined by its liquidus phase boundaries. The construction of eutectic phase diagrams is therefore very relevant to the application of eutectic mixtures. Nonetheless, reliable solid–liquid equilibrium (SLE) phase behavior data on DESs are scarce,[11] partly because eutectic melts were only considered as liquid solvent media since the beginning of this century. Other explanations for this scarcity are the often high viscosity (>100 mPa s at ambient temperature)[12] and hygroscopicity[13] of DESs. These properties complicate sample handling and reduce the reproducibility of phase behavior data. Moreover, many eutectic systems show significant supercooling,[14–16] which interferes with the recrystallization that is required for the determination of the liquidus phase boundary using dynamic analysis techniques.

Most commonly, the solidus and liquidus temperatures are analyzed with differential scanning calorimetry (DSC).[17–19] Other calorimetric and optical analysis techniques [such as hot-stage microscopy (HSM) and melting point apparatus] can be used as well.[13,20] Using these dynamic techniques, the temperature of a mixture with a known composition is varied, while its phase state is detected. Figure 1 shows a typical phase diagram of a eutectic mixture. Steps I–III (red path) illustrate how a sample undergoes various phase transitions upon melting using dynamic analysis techniques. Typically, an initial heating step is applied in order to homogenize the sample (I). The liquid mixture is subsequently cooled below the solidus temperature (II) to induce crystallization and to form a uniform solid phase composed of immiscible solids A and B. However, many DESs do not crystallize within time scales practical for dynamic analysis; some mixtures only crystallize after several days or longer.[21] Instead, they are supercooled towards a metastable liquid phase and eventually towards the amorphous solid state (glass). Many DESs were categorized as low

[a)]Authors to whom correspondence should be addressed: a.c.c.esteves@tue.nl, Tel.: +31(0)402473034 and a.v.d@bruinhorst.com, Tel.: +31 (0)402478246.
[b)]Present address: Department of Chemical Engineering, Khalifa University of Science and Technology, Petroleum Institute, P.O. Box 2533, Abu Dhabi, United Arab Emirates.

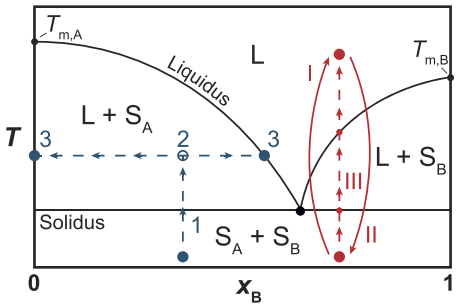

FIG. 1. Schematic representation of a eutectic two-component phase diagram. The red arrows illustrate typical temperature paths when applying dynamic techniques. A mixture (x_B) is (I) heated until all solid has melted, (II) cooled below solidus T for crystallization, and (III) heated until all solid has melted while following phase transitions. Cooling/heating rates are fixed, and steps (II) and (III) can be repeated. The blue arrows illustrate the equilibrium-based approach: a mixture (x_B) is (1) heated to a known T, (2) left at that T for sufficient time to reach equilibrium, and then (3) the liquid and solid phases are separated isothermally and their compositions are determined.

transition temperature mixtures, only showing a glass transition temperature with DSC.[22] Glass formation is especially enhanced close to the eutectic point.[14–16] Hence, dynamic analysis techniques are not always suitable to study the liquid range of DESs and other eutectic mixtures.

The crucial crystallization step can be avoided when using the experimental procedure explored in this paper: the centrifuge method. Following this method, the mixture is only *partially* liquefied and kept at a constant temperature within the L + S region of the phase diagram (Fig. 1, blue path, step 1). After reaching thermodynamic equilibrium between the solid and liquid phase, the phases are separated through centrifugation (Fig. 1, blue path, steps 2–3). A point on the liquidus phase boundary is then obtained via composition analysis of the liquid phase (typically the top phase). In principle, any other S–L phase separation technique could be applied, such as sedimentation and filtration. However, the high viscosity exhibited for most DESs leads to long sedimentation times (gravity only) and high filtration pressures or filter clogging. Hence, accelerated sedimentation by centrifugation was considered as the most appropriate technique for S–L phase separation after equilibration.

The formed liquid can only be considered in equilibrium with the solid phase when the components are homogeneously dissolved in both phases and the phases are in full contact. Hence, the initial solid mixture should be homogenized prior to measurement, for instance, through grinding. The mixtures cannot be considered homogeneous on a molecular level when using a pestle and mortar. For simple eutectic mixtures, this suffices because the liquid formed at the interface between the two solid components is believed to facilitate further liquefaction,[23] allowing the mixture to reach equilibrium with the pure solids. Usually, binary mixtures of organic compounds do not form solid solutions.[24] When a eutectic mixture does form solid solutions, more extensive pretreatment techniques like ball-milling[25,26] are required to achieve a homogeneous solid phase before the measurement. Another option would be to melt the mixture completely at temperatures above the liquidus phase boundary followed by recrystallization of the sample over a time period sufficient to solidify the mixture. For systems showing a strong supercooling tendency, this could be rather time-consuming.

Centrifuges have been used before to study eutectic systems. Metal alloys[27,28] and binary mixtures of molten salts[29–31] have been studied in tailor-made centrifugal setups that could operate at high temperatures. The high temperature complicates sampling of the liquid phase; hence, the mixtures are typically quenched or (rapidly) cooled followed by composition analysis of the resulting solid phases. For metals and high-melting temperature salts, quenching is an option because supercooling or vitrification occurs at high cooling rates only, except for some very specific multicomponent (4 to 5 components) mixtures and alloys.[32]

The aim of this work is to verify whether the equilibrium-based centrifuge method can be used to study the liquidus phase boundary of binary eutectic systems. As a reference system, the binary mixture of 1,2–diphenylethane (bibenzyl) and 1,1′–biphenyl (biphenyl) was selected. This binary system shows ideal eutectic phase behavior between 302 and 342 K,[33] which is largely within the temperature range of the employed centrifuge equipment (263–333 K). Furthermore, the phase diagram of the biphenyl–bibenzyl system could be reconstructed and verified with DSC since it is not sensitive to supercooling. The method was thereafter also applied to a eutectic system that is sensitive to supercooling: the urea–choline chloride mixture, one of the first reported DESs.[1] This centrifuge method, upon successful verification, offers a powerful alternative to construct the liquidus phase boundaries of DESs, particularly of the ones which are hard to quantify owing to strong supercooling behavior.

II. MATERIALS AND METHODS

A. Chemicals

Urea and choline chloride (ChCl) were dried for >48 h under high vacuum and stored under a dry nitrogen atmosphere before use. Table I shows the chemicals used in this work, including their supplier, the CAS number, and purity (as stated by the supplier). Biphenyl and bibenzyl showed a significantly lower melting point than those reported in the literature. For that reason, they were slowly recrystallized for several hours at ambient temperature from warm ethanol (318 K). Subsequently, the crystals were filtrated under vacuum and washed with cold ethanol (to prevent dissolving of the crystals). Residual ethanol was removed in 4–8 h using a rotary evaporator at ~175 mbar and 333 K for bibenzyl and 348 K for biphenyl, respectively. The pure molten bibenzyl and biphenyl

TABLE I. Chemicals used for the reconstruction of the biphenyl–bibenzyl and urea–choline chloride phase diagrams.

Chemical	Supplier	CAS	Purity[a] (wt. %)
Biphenyl	Sigma–Aldrich	92-52-4	99.7
Bibenzyl	Sigma–Aldrich	103-29-7	99.6
Urea	Sigma–Aldrich	57-13-6	99.6
Choline chloride	Sigma–Aldrich	67-48-1	99.3
Ethanol (absolute, AR)	Biosolve B.V.	64-17-5	>99.9

[a]As stated in the certificate of analysis by the supplier.

were recrystallized at room temperature and ground to a fine white powder using a mortar and pestle; their melting points were evaluated with DSC. This procedure was repeated until the melting point was in agreement with previously reported values in the literature.

B. Sample preparation, equilibration, and separation

A graphical representation of the centrifuge method is shown in Fig. 2.

Binary mixtures with a total weight of 6 g were ground with a mortar and pestle at the aimed compositions under dry nitrogen atmosphere, inside a glove box. For the biphenyl–bibenzyl system, six different compositions on both sides of the eutectic composition were prepared (see Table II). For urea–ChCl, the compositions were selected at which the liquidus temperature falls within the temperature range of the centrifuge, as estimated from literature data.[13,34]

The solid mixture was added to a 10 ml centrifuge tube (length 90 mm, inner diameter 14 mm). The tubes were sealed with a cap equipped with an integrated temperature logger (resolution 0.1 K, accuracy ±0.2 K, precision ±0.1 K) custom-made by Avular B.V. Eindhoven, The Netherlands. It was ensured that the sensor tip of the temperature logger was immersed at least 5 mm into the mixture throughout the experiment before sampling.

Equilibration was done outside the centrifuge in a thermostated aluminum heating block regulated by an IKA RCT basic hot plate equipped with an ETS D-5 controller (accuracy ±0.5 K, precision 0.1 K) for ≥30 min. The centrifuge (Sigma 2-16KHL, temperature range 263–333 K, resolution of 1 K) showed systematic over- and under-heating; see Sec. A of the supplementary material. The samples were centrifuged at the aimed temperature for 30 min at 3500 rpm. The mixture's temperature was logged during equilibration and centrifugation for the biphenyl–bibenzyl system and measured after centrifugation with a pre-heated Pt100 sensor for the urea–ChCl system. After centrifugation and temperature analysis, a sample (10–50 mg) of the liquid (top phase) was taken with a Finn-pipet with a plastic tip for composition analysis with ^{1}H-NMR. The insulating properties of the plastic tip retarded the cooling of the sample and prevented crystallization during sampling (only relevant for the biphenyl–bibenzyl mixtures).

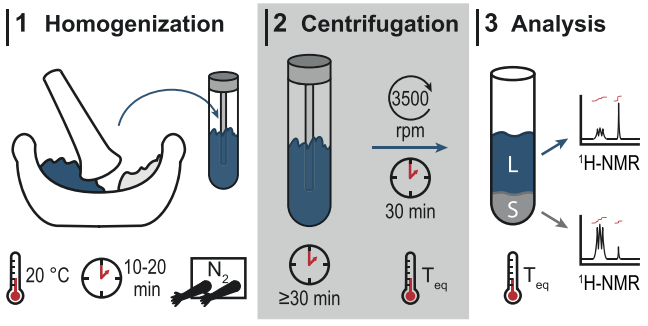

FIG. 2. Graphical representation of the steps involved with the centrifuge method.

TABLE II. Overview of the initial molar biphenyl ($x_{bip,ini}$) and urea ($x_{urea,ini}$) fractions used for the centrifuge method and the temperatures set at the centrifuge (T_{set}).

$x_{bip,ini}$	T_{set} (K)	$X_{urea,ini}$	T_{set} (K)
0.05	318	0.50	333
0.15	314	0.50	328
0.20	309	0.55	323
0.25	305	0.55	318
0.30	302	0.55	313
0.35	301	0.55	308
0.55	301	0.55	303
0.60	305	0.75	303
0.66	313	0.75	308
0.75	318	0.75	313
0.82	328	0.75	318
0.88	333	0.75	323
		0.75	333
		0.80	328
		0.80	333

C. DSC analysis

A TA instruments DSC Q2000 equipped with a standard cell, flushed with nitrogen (50 ml min^{-1}), and a liquid nitrogen cooling system (LNCS) was used for DSC analysis. The cell constant calibration and validation were performed with high purity indium (>99.95%) as a reference standard. The temperature calibration was done with high purity indium and cyclohexane (>99.9%, melting and solid–solid transition). An empty aluminum hermetic Tzero pan was used as the reference pan. The heat capacity calibration was performed with a 26.308 mg synthetic sapphire disk crimped into a hermetic Tzero pan matching the weight of the reference pan within 50 μg. Samples of 5–7 mg were added to a hermetic Tzero pan. All thermograms were analyzed using the Universal Analysis software package (version 4.5A). The composition of the samples containing the binary mixtures of interest was determined with ^{1}H-NMR spectroscopy after DSC analysis. To this aid, the DSC pan was punctured and its content was dissolved in the appropriate deuterated solvent. The accuracy of the temperature, enthalpy, and heat capacity was estimated at 0.05 K, 2%, and 3%, respectively, determined from verification runs of the calibration standards. The precision of the onset and peak temperatures was 0.1 K and 0.5 K, respectively. The precision of the enthalpy and heat capacity was 3% and 5%, respectively.

1. Thermal properties of pure biphenyl and bibenzyl

In order to determine the melting temperature and melting enthalpy, the bibenzyl samples were heated at a rate (β) of 1 K min^{-1} from 303 to 333 K and cooled at the same rate for at least two cycles (see Sec. B of the supplementary material for the selection of the heating rate). The biphenyl samples were heated at β = 1 K min^{-1} from 323 K to 353 K and cooled at the same rate for at least two cycles. For both components, the onset temperature of the melting peak was taken as melting temperature. The enthalpy was calculated from the integral of the melting peak.

The liquid- and solid-phase molar heat capacities of biphenyl and bibenzyl were measured using a modulated temperature program for the DSC. The sample was equilibrated at 253 K; then, the sample was heated to 373 K with an average heating rate of 1 K min^{-1} and a temperature modulation of ±0.2 K per 120 s. The molar heat capacity was calculated from the specific reversing heat capacity and the molar mass of the compound of interest. The data were recorded for at least two samples and then averaged.

2. Analysis of the solidus and liquidus temperature

The biphenyl–bibenzyl mixtures were subjected to the heating programs listed in Table III. The onset of the first peak in the resulting thermograms was taken as solidus (eutectic) temperature, and the maximum of the second peak was taken as liquidus temperature (see Sec. B of the supplementary material for the rationale behind the peak event selection). The peak maximum was determined as the maximum of the heat flow signal. However, in the case of a shoulder or a second peak in the liquidus DSC signal, the last minimum of the second derivative of the heat flow was taken as peak maximum (supplementary material, Sec. B).

D. Composition analysis with ^{1}H-NMR spectroscopy

Biphenyl–bibenzyl mixtures were dissolved in approximately 1 ml $CDCl_3$ with 3 v/v% tetramethylsilane (TMS) as the internal standard, while the urea–ChCl mixtures were dissolved in DMSO-d_6. The resulting solution was then transferred to a 5 mm thin-walled economic Wilmad NMR tube. The tube was capped and sealed with Parafilm® to avoid solvent evaporation. A Bruker 400 MHz spectrometer equipped with an autosampler carrousel was used for ^{1}H-NMR spectroscopy. The spectra were recorded using 16 scans with a relaxation time of 5 s between the RF pulses, and the spectra were auto-shimmed and auto-phased by the Bruker TopSpin® software used to control the equipment. The peaks were manually integrated using MestReNova 10.0.2, after applying a Withaker Smoother baseline correction and small phase corrections if necessary. The molar ratio of biphenyl–bibenzyl and urea–ChCl was calculated from these integrals, as described in Sec. C of the supplementary material, where it is also explained how the accuracy and precision of the composition analysis depend on the molar ratio of the studied mixture.

TABLE III. Heating steps applied in the DSC heating program. Quantity β is the heating rate of interest, and steps 2–6 and 2–5 were repeated for heating rates $0.5 \le \beta \le 2$ K min^{-1} and $5 \le \beta \le 10$ K min^{-1}, respectively.

Step	$0.5 \le \beta \le 2$ K min^{-1}	$5 \le \beta \le 10$ K min^{-1}
1	Heat to 373 K at 20 K min^{-1}	Heat to 373 K at 20 K min^{-1}
2	Equilibrate at 373 K for 10 min	Equilibrate at 373 K for 10 min
3	Cool to 253 K at 20 K min^{-1}	Cool to 253 K at 20 K min^{-1}
4	Equilibrate at 253 K for 5 min	Equilibrate at 253 K for 5 min
5	Heat to 293 K at 20 K min^{-1}	Heat to 373 K at β K min^{-1}
6	Heat to 373 K at β K min^{-1}	

III. RESULTS AND DISCUSSION

A. Pure components of the reference system

In order to verify the purity of the recrystallized bibenzyl and biphenyl, their melting temperatures and enthalpies were compared to literature data. As shown in Table IV, the bibenzyl and biphenyl melting temperature and enthalpy of fusion agree with their corresponding literature values after recrystallization. Two batches of bibenzyl were recrystallized, showing no significant differences in melting behavior.

With modulated DSC, the heat capacity was recorded upon heating, providing a continuous $C_{p,m}$ signal as a function of temperature.[39] These data were fitted to a second order polynomial for both the solid and liquid phases using the following equation:

$$C^{j}_{p,m,i} = \mathrm{A} \cdot T^2 + \mathrm{B} \cdot T + \mathrm{C}, \tag{1}$$

where $C^{j}_{p,m,i}$ is the heat capacity of component i in phase j in J (mol K)$^{-1}$ and T is the temperature in K. In Sec. D of the supplementary material, the fitting constants A, B, and C and the adjusted coefficients of determination are presented. Tables V and VI compare the molar heat capacities of biphenyl and bibenzyl obtained in this work to those available in the literature at various temperatures. The values presented in this work are the averaged values of duplicate measurements. It follows that our measured heat capacities are in good agreement with the literature values.

B. Construction of the reference phase diagram with DSC

The SLE phase diagram of the biphenyl–bibenzyl system was reconstructed using DSC. This was done in order to confirm the measured phase diagram presented in 1935 by Lee and Warner.[33] The liquidus phase boundaries of a simple eutectic system—i.e., complete miscibility in the liquid phase and complete immiscibility in the solid phase—can be described thermodynamically,[2,40] using

$$\ln x^L_i \gamma^L_{x,i} = \frac{\Delta_{\mathrm{fus}} H^*_{m,i}}{R}\left(\frac{1}{T^*_{\mathrm{fus},i}} - \frac{1}{T}\right) - \frac{1}{RT}\int_{T^*_{\mathrm{fus},i}}^{T} \Delta^L_S C^*_{p,m,i}(T)dT + \int_{T^*_{\mathrm{fus},i}}^{T} \frac{\Delta^L_S C^*_{p,m,i}(T)}{RT} dT, \tag{2}$$

TABLE IV. Experimental melting temperatures and molar enthalpies of fusion of bibenzyl and biphenyl as supplied (commercial), after purification (recrystallized), and those reported in the literature. Data of the second batch (b2) of recrystallized bibenzyl are presented separately.

	Bibenzyl		Biphenyl	
Source	T^*_{fus} (K)	$\Delta_{\mathrm{fus}} H^*_m$ (kJ mol^{-1})	T^*_{fus} (K)	$\Delta_{\mathrm{fus}} H^*_m$ (kJ mol^{-1})
Commercial	322.19	21.76	341.88	17.56
Recrystallized	324.48	22.75	342.41	18.57
Recrystallized (b2)	324.57	22.49		
Literature	324.40[33]	22.73[35]	342.2[33]	18.576[36]
	324.348[35]		342.10[36]	18.58[37]
			342.20[37]	18.8[38]

TABLE V. Measured molar heat capacities ($C_{p,m}$) and standard deviations ($\delta C_{p,m}$) at various temperatures of recrystallized biphenyl and those reported in the literature.

	This work		O'Rourke and Mraw[37]		Chirico *et al.*[36a]
	$C_{p,m}$	$\delta C_{p,m}$	$C_{p,m}$	$\delta C_{p,m}$	$C_{p,m}$
T (K)	J (mol K)$^{-1}$	J (mol K)$^{-1}$	J (mol K)$^{-1}$	J (mol K)$^{-1}$	J (mol K)$^{-1}$
			Solid		
260	172.1	9.3	169.4	1.9	170.7
280	185.2	8.7	184.1	1.6	185.3
300	199.8	9.0	199.7	1.0	199.7
320	213.4	9.1	212.7	...[b]	215.1
			Liquid		
350	268.1	8.9	271.0	...[b]	273.0
360	272.4	10.2	275.3	...[b]	277.3
370	276.2[c]	10.2	280.8	...[b]	281.5

[a]Estimated uncertainty was 1% for all values.
[b]One value reported.
[c]Recorded at 269.62 K.

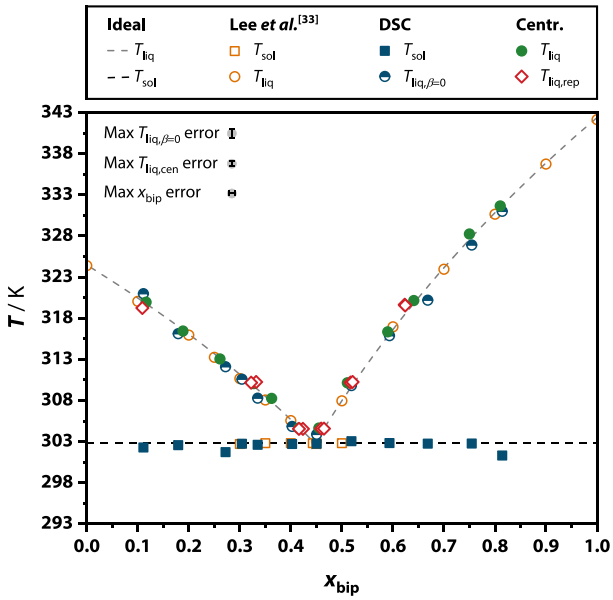

FIG. 3. Solidus and liquidus temperatures (T_{sol} and T_{liq}) of the ideal biphenyl–bibenzyl mixture, data obtained from the literature[33] (Lee and Warner), samples measured by DSC, and samples measured with the centrifuge method (Centr.). Subscript rep corresponds to repetitions and subscript $\beta = 0$ corresponds to extrapolated to zero heating rate. In the upper-left corner, the maximum error of the data caused by the inaccuracy and standard deviation of the analysis methods is depicted. The error bars are smaller than the symbol size and are therefore not displayed.

where x_i^L is the mole fraction of component i in the liquid phase, $\gamma_{x,i}^L$ is the activity coefficient of component i in the liquid phase, $\Delta_{fus}H_{m,i}^*$ is the molar enthalpy of fusion of pure i, R is the gas-constant, $T_{fus,i}^*$ is the melting temperature of pure i, T is the temperature of the mixture, and $\Delta_S^L C_{p,m,i}^*(T)$ is the difference between the solid and liquid molar heat capacity at constant pressure of pure i. At the hypotectic side, (2) describes the equilibrium between pure solid bibenzyl and the liquid mixture, while at the hypertectic side, this is the equilibrium between pure solid biphenyl and the liquid mixture.

In Fig. 3, the DSC data, the literature dataset, and the results from the centrifuge method are presented together with the two ideal liquidus boundaries ($\gamma_{x,i}^L = 1$). Both the liquidus and solidus temperatures obtained by DSC are in good agreement with those presented by Lee and Warner[33] and follow a trend that is nearly ideal. For the liquidus temperatures, the best results were obtained with the peak maxima that were extrapolated to the equilibrium condition of zero heating rate ($\beta = 0$). A more detailed discussion on the extrapolation and the heating rate dependency of the thermograms is given in Sec. B of the supplementary material. The ideal liquidus boundaries were constructed with (2), using the measured $\Delta_{fus}H_{m,i}^*$, $T_{fus,i}^*$, and fitted $\Delta_S^L C_{p,m}(T)$ of the recrystallized pure components as input (see Table IV and Sec. D of the supplementary material). The intersection of the two liquidus curves was taken as the eutectic point. The solidus phase boundary was drawn as a horizontal line through this eutectic point.

The polynomial fits of the experimental $C_{p,m}$ data obtained by DSC were used to determine the $\Delta_S^L C_{p,m}(T)$ term in (2), yielding a solidus and liquidus phase boundary that matches the literature data and DSC data very well. The impact of $\Delta_S^L C_{p,m}(T)$ on the ideal eutectic composition and temperature is shown in Table VII. It can be seen that the $\Delta_S^L C_{p,m}(T)$ has a significant effect on the position of the eutectic point and that the phase boundaries calculated from the experimental data match those calculated from literature data.

TABLE VI. Measured molar heat capacities ($C_{p,m}$) and standard deviations ($\delta C_{p,m}$) at various temperatures of recrystallized bibenzyl and those reported by Messerly *et al.*[35] (Ref).

	This work		Ref[a]
T (K)	$C_{p,m}$ J (mol K)$^{-1}$	$\delta C_{p,m}$ J (mol K)$^{-1}$	$C_{p,m}$ J (mol K)$^{-1}$
	Solid		
260	220.2	13.6	218.3
270	228.4	13.7	227.3
280	236.8	13.5	236.4
290	245.1	14.5	245.8
300	255.9	13.4	255.5
310	264.9	13.8	265.0
	Liquid		
335	323.4	14.3	318.4
340	325.8	14.2	321.4
345	328.3	14.8	324.3
350	331.9	14.9	327.1

[a]Estimated uncertainty was 0.1% for all values.

TABLE VII. The influence of the heat capacity difference between the solid and liquid phase of pure biphenyl and bibenzyl as a function of temperature ($\Delta_S^L C_{p,m}(T)$) on the eutectic composition (mole fraction of biphenyl, $x_{bip,eut}$) and temperature (T_{eut}) calculated from ideal eutectic phase behavior.

	$x_{bip,eut}$	T_{eut} (K)
No $\Delta_S^L C_{p,m}(T)$ contribution	0.439	303.67
$\Delta_S^L C_{p,m}(T)$ from DSC data	0.446	302.84
$\Delta_S^L C_{p,m}(T)$ from literature data	0.447	302.80

Figure 4 shows that the DSC thermograms (heat flow as a function of temperature) exhibit typical eutectic behavior. The first S–L phase transition—the eutectic peak—is sharp and reaches a maximum at $x_{bip} = 0.446$, the eutectic composition. The second peak is broad, showing an exothermic signal from the end of the eutectic peak until the liquidus phase boundary is reached.

For compositions approaching the pure components, the onset temperature of the solidus peak tends to be lower than the eutectic temperature. This could be attributed to the formation of a solid solution of small amounts of biphenyl in bibenzyl, and vice versa. For solid solutions, a second phase transition at a higher temperature would be expected. The solid solution then partially melts into the liquid, but this was not observed. Alternatively, the observed lower solidus temperatures could be explained by the effect of the peak shape of the solidus transition at the onset temperature. The solidus peak becomes very small in the regions near the pure components, resulting in a less steep signal increase, which leads to a possible underestimation of the onset temperature. This phenomenon is graphically depicted in Fig. 5.

From the integral of the solidus peak, the melting enthalpy of the eutectic mixture can be determined. The melting enthalpy of the solidus transition has its maximum at the eutectic composition and decreases linearly with composition towards the pure components. The eutectic composition therefore lies at the intersection of the linear fits of the hypotectic and hypertectic data points in the Tammann-plot; see Fig. 6. The eutectic composition obtained from the Tammann-plot ($x_{bip} = 0.459$) is slightly higher than the ideal eutectic composition ($x_{bip} = 0.446$) and the value reported in the literature ($x_{bip} = 0.443$). The most probable explanation is that the end point of the solidus peak overlaps with the liquidus peak, complicating accurate integration. At the hypotectic side, large variations (10%–20%) were observed that tilted the linear fit, but those could not be labeled as outliers from the residual plots. Taking the unknown accuracy into account, the deviation of the eutectic composition (~2.8%) was considered acceptable.

In conclusion, the eutectic diagram of the biphenyl–bibenzyl system obtained from the DSC data closely matches the phase diagram measured by Lee and Warner[33] and can be predicted accurately when assuming ideal behavior. For these reasons, the biphenyl–bibenzyl mixture is a very suitable reference system.

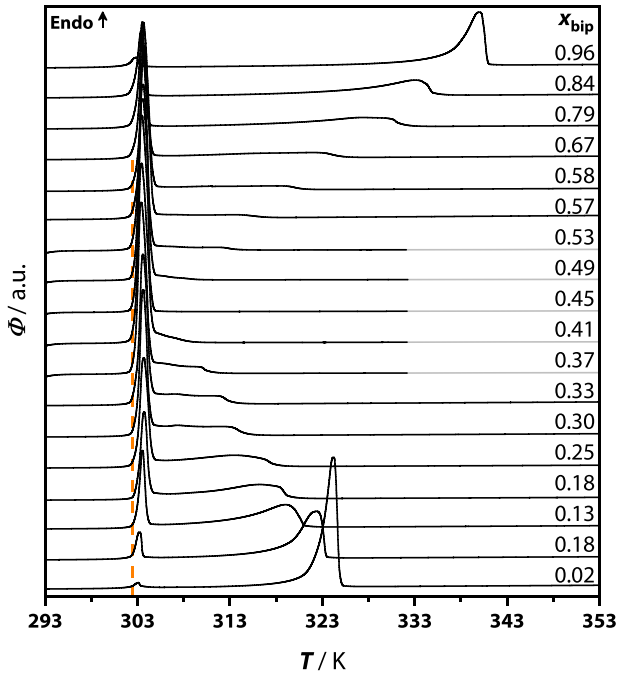

FIG. 4. Stacked DSC thermograms on heating (heating rate is 1 K min^{-1}) for various biphenyl–bibenzyl mixtures with molar fraction x_{bip}, where Φ is the heat flow. The endothermic peaks (up) correspond to eutectic (first peak, onset marked with orange dashed line) and liquidus (second peak) melting. Only the last step of the DSC program is shown, as this step was used to construct the liquidus phase boundary. The gray lines are extrapolations from the baseline as those samples were run up to 333 K.

C. The centrifuge method

1. Validation of the centrifuge method

The results collected in Fig. 3 clearly show that the centrifuge method SLE data are very close to the liquidus phase boundary constructed earlier[33] and by DSC (this work). It should be noted that the data presented in Fig. 3 were obtained via an optimized experimental procedure for the equipment used in this study. The optimization is reproduced in Sec. III C 2 in order to highlight common sources of systematic errors and approaches that can improve the repeatability, accuracy, and precision of the experiment. Considering the very good agreement of the data shown in Fig. 3, the optimized centrifuge method can be regarded as a valid method for the analysis of S–L phase boundaries of eutectic mixtures.

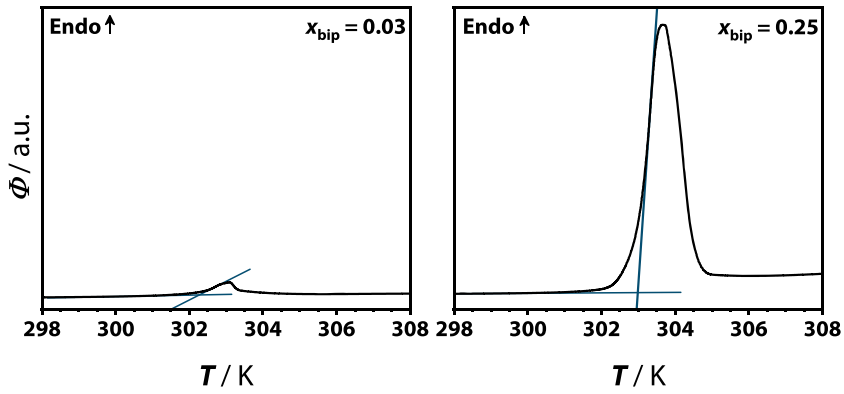

FIG. 5. The extraction of the onset temperature from the thermograms (endotherms up, Φ is the heat flow) of two samples with (left) a molar biphenyl fraction (x_{bip}) of 0.03 and (right) of 0.25, using the intersection between the tangents in the inflection point of the peak front and the tangents of the baseline. The onset temperature was significantly lower for $x_{bip} = 0.03$ than for $x_{bip} = 0.25$.

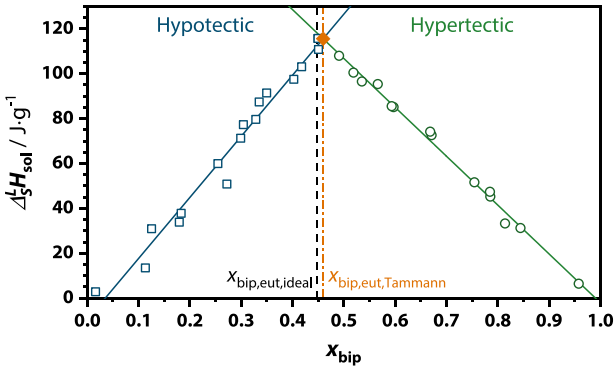

FIG. 6. Tammann-plot constructed from the enthalpies of the solidus peak $\Delta_S^L H_{sol}$ in the DSC thermograms obtained for the biphenyl–bibenzyl system. $\Delta_S^L H_{sol}$ data were obtained from the solidus peak integral of thermograms that were recorded at a heating rate of 1 K min^{-1}. The eutectic composition determined for an ideal biphenyl–bibenzyl system (black dashed line) and obtained from the Tammann-plot (orange dashed–dotted line) is highlighted.

2. Experimental optimization

Within the centrifuge method, four main steps can be distinguished:

(1) Mixing of the pure components and homogenization of the mixture;
(2) equilibration of the mixture at the aimed temperature;
(3) phase separation through centrifugation at the aimed temperature;
(4) composition and temperature analysis of the liquid top phase.

Following the first step, biphenyl and bibenzyl were ground together. If the mixture of interest is prone to co-crystallization or solid solution formation, more extensive homogenization or pretreatment steps might be required; see Sec. III D and Sec. F of the supplementary material. For the ideal eutectic biphenyl–bibenzyl system, grinding was sufficient and it resulted in a fine and dry powder that was easy to handle. The solid mixture was then transferred into a centrifuge tube for the second step. The centrifuge manufacturer only guarantees a homogeneous temperature throughout the centrifuge when the rotor is spinning, but phase separation is only desirable *after* equilibration. Hence, the mixture was equilibrated *outside* the centrifuge to avoid temperature fluctuations. Meanwhile, the centrifuge was brought to the aimed temperature by spinning the rotor without samples. The third step comprises the separation of the phases through centrifugation. Pictures of the phase separated mixtures and those before and after equilibration are presented in Fig. 7.

After centrifugation, the fourth step was carried out: the measurement of temperature and composition of the liquid phase. Initially, a small sample was taken for composition analysis, followed by the immersion of a Pt100 temperature sensor. It took 2–10 min for the sensors to stabilize at the temperature of the liquid. This allowed the mixtures to cool down during analysis. Moreover, at high temperatures, it took longer to measure a stable temperature than at low temperatures. The different stabilization times of the Pt100 sensor introduced a potential error between the measurements. Figure 8 shows how this method (Pt100) resulted in different compositions at seemingly similar temperatures. The fact that most liquidus temperatures in the hypotectic region are lower than the ideal liquidus phase boundary probably originates from the formation of crystals on the temperature probe. The temperature probe, which is initially at room temperature, acts as a cold sink for the bibenzyl in the liquid top phase and initiates crystallization. An insulating layer of small crystals could be observed on the probe.

In order to avoid crystallization upon sensor immersion and to shorten the sensor stabilization times, the Pt100 sensors were pre-heated at the aimed temperature in an aluminum block. As shown in Fig. 8, this significantly improved the data. However, the set centrifuge temperature was generally not matching the measured temperature in the liquid top-phase after centrifugation. Therefore, custom-made temperature loggers were developed by Avular B.V., which allowed for the evaluation of the temperature during equilibration (second step) and centrifugation (third step).

From the obtained temperature profiles [e.g., Fig. 9(a)], it can be concluded that the centrifuge temperature control overheats the mixtures. Since the heating block did reach and maintain the set temperature, the mixtures needed time to acclimatize when switched to the higher temperature at the centrifuge. This might influence the results. Therefore, the relation between the set temperature and the actual temperature of the mixture was determined over the temperature range of the centrifuge (supplementary material, Sec. A). Figure 9(b) shows that the temperature difference between equilibration and centrifugation is reduced and a constant temperature is reached and maintained at an earlier stage during centrifugation. However, after the transfer of the tubes to the centrifuge, the temperature shows a rise or drop. This could not be reduced by a quicker transfer (a few seconds vs. a minute) from the heating block to the centrifuge. It appeared that opening the lid of the centrifuge activates the temperature control of the centrifuge, causing an initial drop or even a rise in temperature. The temperature fluctuations can lead to extra crystal or

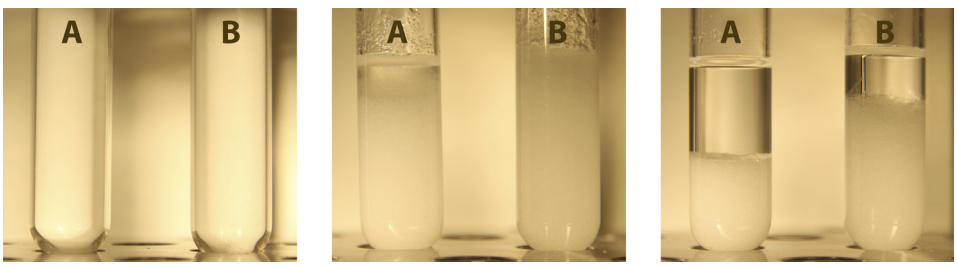

FIG. 7. Pictures of biphenyl–bibenzyl mixtures with molar biphenyl ratios of 0.20 (A) and 0.70 (B) after the different steps of the centrifuge method: (left) after mixing, (middle) after equilibration, and (right) after centrifugation.

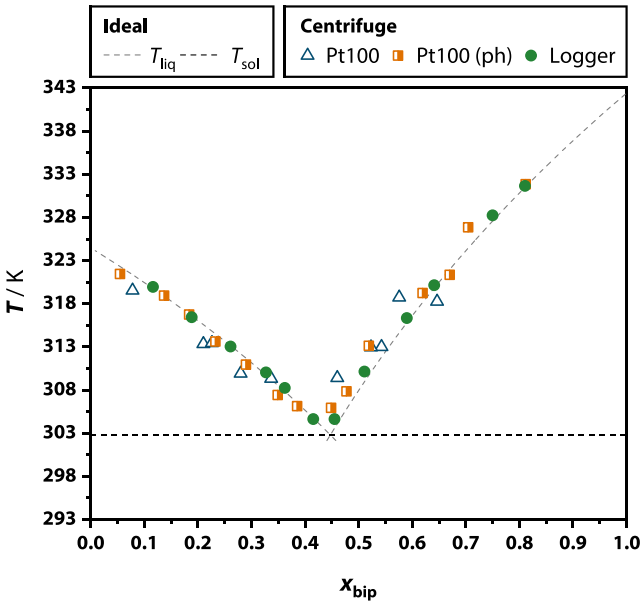

FIG. 8. *T*–*x* phase diagram of the biphenyl–bibenzyl system, based on ideal eutectic behavior and the centrifuge method. The temperature of the liquid top phase was determined using three different procedures: (i) immersing a Pt100 sensor after centrifugation; (ii) the same as (i) with preheated (ph) Pt100; (iii) logging the temperature throughout the whole experiment. Subscripts liq and sol stand for liquidus and solidus transition, respectively.

liquid formation. The latter would lead to an over-estimation of the liquefaction of the solid component since the solids that were liquefied during a temperature rise will not recrystallize when the system shows strong supercooling behavior.

The temperature drop could not be avoided since the lid needs to be opened to transfer the samples into the centrifuge. Therefore, an additional static equilibration step was introduced for the samples that were inserted to the centrifuge, which allows the mixture to reach a stable temperature prior to rotation. As mentioned before, the temperature of the centrifuge in the spinning state differs from that in the static state. Hence, an additional temperature calibration had to be performed that correlates the aimed temperature to the actual temperature in the centrifuge after keeping the rotor static for 1 h (supplementary material, Sec. A). The set centrifuge temperature needed to be changed after static equilibration in order to maintain the same temperature during rotation. Similar to the moment of opening the centrifuge's lid, the temperature control of the centrifuge would induce a drop in temperature if the rotation was started immediately after changing the set temperature. This effect was less pronounced when a little time period (~1 min) was added between setting the temperature for rotation and starting the rotor. Finally, temperature profiles were obtained that all converged to the aimed temperature with a difference of at most 1 K between the external heating block temperature and the end-point centrifuge temperature during rotation (see Fig. 10). After rotation and removal of the sensor, the centrifuge tubes were maintained in the warm centrifuge bucket for the sampling of the liquid phase. The sampling (fourth step) was done as soon as possible after centrifugation and typically within 60 s after the temperature logger was removed from the sample. The average of the last 12 recorded temperatures (2 min) before sampling was taken as liquidus temperature.

In the literature, it has been shown that centrifuged eutectic mixtures are not necessarily homogeneous.[27,41] Hence, the sampling height could affect the measured composition. This introduces measurement errors, but also raises the question of which sampling height would represent the liquid in equilibrium with the solid phase. The inhomogeneity of the mixtures was evaluated in order to check whether the sampling height affects the composition analysis.

An inhomogeneous liquid top phase after centrifugation is most likely to show a concentration gradient over the height of the tube because that is the direction of the applied centrifugal force field. Therefore, the liquid phase was sampled after equilibration and centrifugation at the top of the liquid layer, as well as close to the S–L interface for all mixtures. One sample ($x_{bip,ini} = 0.05$) showed a deviation of $x_{bip} = 0.017$. The liquid layer was very small in this sample, which impeded liquid sampling at different heights without including solids.

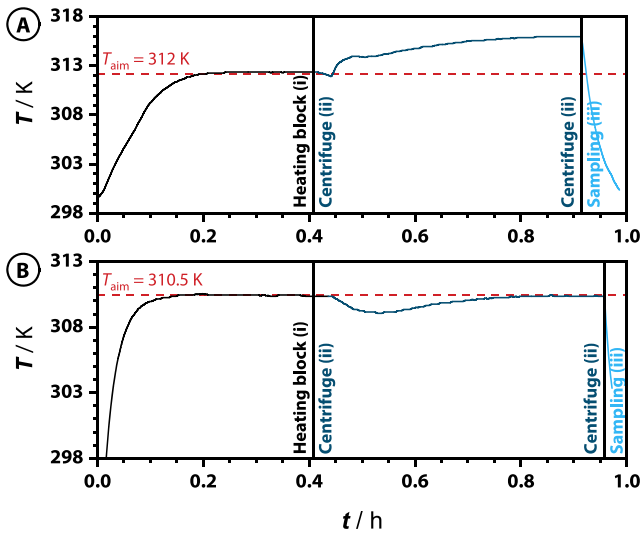

FIG. 9. Typical temperature profiles of mixtures in a centrifuge tube a with temperature logger, where the centrifuge was (a) set at the aimed temperature and (b) set at $T_{aim} - T_{corr}$ (supplementary material, Sec. A). T_{aim} is visualized with a red dashed line. Each profile is divided into three time domains: (i) equilibration in the heating block, (ii) phase separation in the centrifuge, and (iii) sampling of the top phase.

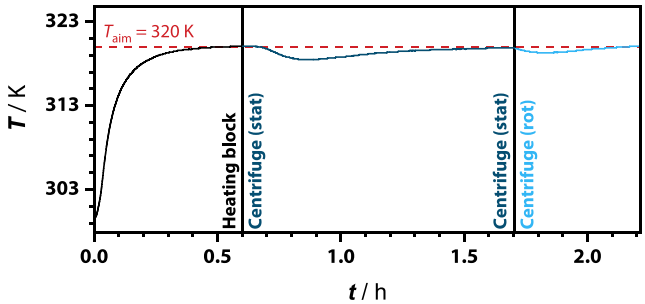

FIG. 10. Temperature profile of the sample with initial molar biphenyl fraction 0.05 in a centrifuge tube with a temperature logger. The profile is divided in three time domains: equilibration in the heating block, equilibration in the centrifuge (stat), and phase separation through rotation (rot) in the centrifuge. The centrifuge temperature was set according to the temperature calibration presented in Table A.1.

For the other samples, the absolute difference in mole fraction between the two sampling heights (Δx_{bip}) was typically in the order of 0.001 without a clear dependency on the sampling height ($\Delta x_{bip} < 0.003$). See Table E.1 (supplementary material, Sec. E) for an overview of the data. The liquid phase of the biphenyl–bibenzyl system can therefore be considered homogeneous.

3. Accuracy, precision, and repeatability

The accuracy and precision of the centrifuge method depend mostly on the temperature and composition analysis. The accuracy and precision of the temperature sensor are stated in Sec. II B. The accuracy of the composition analysis by ^{1}H-NMR was evaluated by preparing and measuring 3 samples with a known composition. The precision was evaluated by measuring and integrating each spectrum 3 times. The results are listed in Table VIII, which shows that the precision as well as the accuracy of the composition improve with increasing biphenyl content. This is the result of the error propagation of the integration errors described in Sec. C.2 of the supplementary material.

The repeatability of the centrifuge method depends on the robustness of the total procedure, which involves all four steps (sample preparation, equilibration, separation, and sampling/analysis). It can best be evaluated by re-preparing and repeating a mixture in a centrifuge tube while keeping all settings constant. Figure 3 shows the data of the repetitions as well as the precision of the analysis method (legend with error bars). The repeated experiments have composition and temperature deviations that slightly exceed the previously discussed precision of the analysis methods.

Most deviations are caused by fluctuations in the mixture's composition. The composition differences do not originate from the liquid sampling because the liquid phase is homogeneous. Hence, multiple samples from the same run resulted in standard deviations within the precisions presented in Table VIII. A possible source of the deviations is the temperature control of the centrifuge, which was not very reliable. Deviations of ±0.8 K as compared to the calibration were observed for the static and the rotating centrifuge. For the repeated experiments, the liquidus temperatures shown in Fig. 3 do not seem to vary. However, those temperatures only represent the endpoint of the temperature program that the sample was subjected to.

Figure 11 shows the temperature profiles of two different samples and their repetitions. These are the samples with the lowest and the highest deviation in composition. The difference in equilibration temperatures at the heating block for the sample with the largest composition deviation ($x_{bip,ini} = 0.25$) was 0.6 K. During centrifugation, the temperatures converge, but the main fraction of the liquid is formed and separated from the solids in the heating block (see Fig. 7). The temperature difference between equilibration and centrifugation was even larger, emphasizing the deviation of the actual temperature from the calibrated temperature. The sample that has the best repeatability shows very similar equilibration and centrifugation temperatures despite the large temperature drop after being inserted to the centrifuge. Most likely, the largest composition deviations arise from different amounts of liquid formed during equilibration. Especially, in systems that are prone to supercooling, the liquid will not recrystallize rapidly and the highest equilibration temperature will determine the liquid composition.

TABLE VIII. Mole fraction of biphenyl of three 2 g batches with different biphenyl–bibenzyl ratios determined by preparation weight ($x_{bip,w}$) and ^{1}H-NMR ($x_{bip,NMR,i}$). From each batch, three ^{1}H-NMR samples were prepared (A–C), which were all measured and integrated three times (1–3). The absolute standard deviation for each ^{1}H-NMR sample (δ_{xbip}) as well as the difference between the average value obtained from ^{1}H-NMR and that calculated from the added weights is shown.

$x_{bip,w}$	Sample	$x_{bip,NMR,1}$	$x_{bip,NMR,2}$	$x_{bip,NMR,3}$	δ_{xbip}	Δx_{bip}[a]
0.101	A	0.105	0.106	0.105	0.0044	0.0047
	B	0.106	0.107	0.106	0.0075	0.0053
	C	0.106	0.105	0.106	0.0044	0.0044
0.541	A	0.544	0.544	0.544	0.0010	0.0027
	B	0.543	0.544	0.543	0.0004	0.0027
	C	0.544	0.544	0.543	0.0008	0.0024
0.900	A	0.900	0.901	0.900	0.0001	0.0002
	B	0.901	0.901	0.901	0.0000	0.0003
	C	0.901	0.901	0.901	0.0001	0.0005

[a] Δxbip = $x_{bip,NMR} - x_{bip,w}$.

D. The centrifuge method applied to the urea–ChCl system

Using the centrifuge method, the eutectic phase behavior of the biphenyl–bibenzyl system could be analyzed. However, this system is not prone to supercooling. The method was therefore also applied to a system that does show significant supercooling, the DES urea–ChCl. Figure 12 shows the results, including existing literature data for this system. The

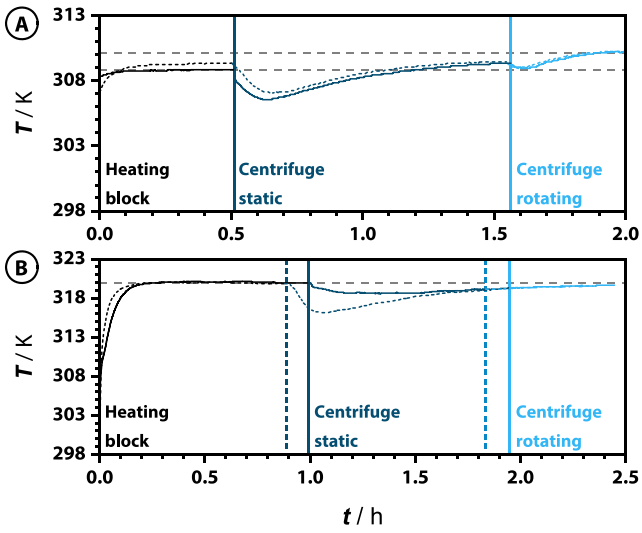

FIG. 11. Temperature profile in time throughout the centrifuge method of biphenyl–bibenzyl mixtures with an initial mole biphenyl fraction of 0.25 (a) and 0.75 (b) at an aimed temperature of 310 and 320 K, respectively. The dashed profiles are repetitions of the solid lines. The vertical lines indicate the start of the three phases of the centrifuge method. The dashed horizontal lines represent the difference between the equilibration and separation temperature.

development of the centrifuge method was initiated to measure the urea–ChCl system. Hence, most data were recorded with pre-heated Pt100 sensors before the temperature loggers were introduced. Two samples were repeated with the optimized method including loggers; the results matched with the trend found with pre-heated Pt100 sensors.

The DSC thermograms presented by Meng *et al.*[13] and Morrison *et al.*[34] confirm that the urea–ChCl system is prone to supercooling. A cold-crystallization peak distorts the baseline, forcing the measurements towards very slow heating rates and lower sensitivities. The supercooling tendency also explains the generally lower liquidus temperatures reported by the initial study of Abbott *et al.* since the data were obtained upon cooling.[1,13] Kim and Park[42] misinterpreted the solid–solid transition of ChCl (~351 K)[43,44] as a liquidus transition. The literature data observed by Meng *et al.*[13] and Morrison *et al.*[34] were therefore considered the most reliable. Hence, the centrifuge method was able to reproduce the liquidus phase boundary reported in the literature at the hypotectic side.

At the hypertectic side, the centrifuge method yields higher liquidus temperatures than those observed in the literature. The liquidus temperatures measured with the centrifuge method prolong the trend observed for the compositions rich in urea ($x_{urea} \geq 0.75$), implying a simple eutectic mixture. A continuous liquidus phase boundary could not be recognized for the literature data in the composition range $0.65 \leq x_{urea} \leq 0.75$; this could be explained by the formation of a co-crystal, as observed by Morrison *et al.*[34] In the current approach, urea and ChCl were ground together and equilibrated at the aimed temperature. For co-crystal formation, the sample should be completely liquefied and recrystallized prior to the measurement. As suggested by Morrison *et al.*,[34] the 2:1 urea–ChCl co-crystal is likely to have a low melting temperature and shows two eutectics close to the stoichiometric composition, one with ChCl and one with urea. They also suggested that formation of the co-crystal can be hampered by an excess of either urea or ChCl. Recrystallization does therefore not necessarily lead to a mixture containing the co-crystal, which could also explain the large differences between the HSM and DSC data at $x_{urea} \approx 0.75$ of Meng *et al.* (Fig. 12).

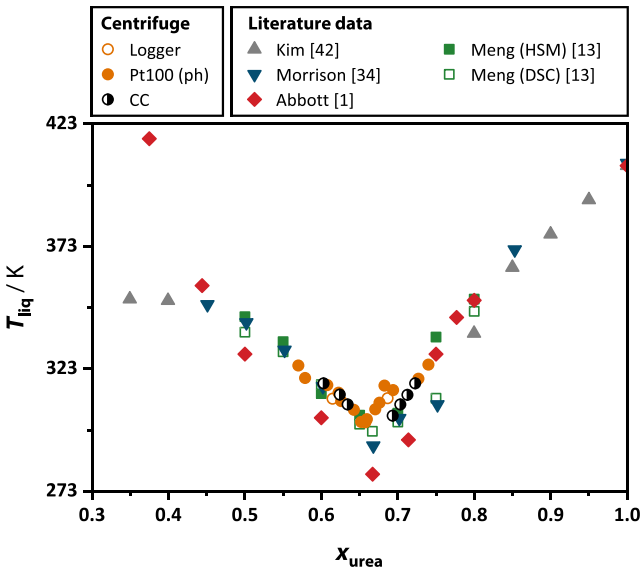

FIG. 12. *T*–*x* phase diagram of the urea–ChCl system. The centrifuge method data were obtained with preheated (ph) Pt100 and a temperature logger. Some samples were prepared by grinding the co-crystal (CC) together with either ChCl (hypotectic) or urea (hypertectic). Meng *et al.* recorded their data with DSC and hot-stage microscopy (HSM);[13] other literature data were reported by Kim and Park,[42] Morrisson *et al.*,[34] and Abbott *et al.*[1]

In order to ensure the presence of the co-crystal, a mixture with $x_{urea} = 0.667$ was melted, recrystallized, and subsequently ground together with urea or ChCl. These samples were then analyzed with the centrifuge method, showing no deviations at the hypotectic side. At the hypertectic side, however, the liquidus phase boundary shifted to lower temperatures (Fig. 12). The centrifuge method data on the urea–co-crystal system are now coinciding with the DSC data from the literature and confirming slightly different eutectic behavior as compared to urea–ChCl mixtures. If co-crystal formation is expected, best would thus be to prepare samples from a solid mixture of co-crystal + one of the pure components or completely recrystallize the samples from the liquid phase prior to the measurement. Solid-solution formation may also contribute to the differences between recrystallized urea–ChCl and a mixture of pure solids; see Sec. F of the supplementary material.

The large differences between the different analysis methods at $x_{urea} \approx 0.75$ are a topic for further investigation. The transition observed with DSC could be studied in more detail at smaller composition intervals or with supplementary analysis techniques such as X-ray scattering.

IV. CONCLUSIONS

The phase behavior of biphenyl–bibenzyl mixtures described in the literature was confirmed with DSC and can be easily predicted theoretically because it behaves ideally. This system was used to validate the centrifuge method, an alternative equilibrium-based method to study the liquidus phase boundaries of eutectic systems. Liquidus temperatures obtained with the centrifuge method match the literature data. For the biphenyl–bibenzyl system, the largest deviations originated from the poor temperature control of the commercial centrifuge used in this study. Hence, the quality of the data could probably be further improved by using a centrifuge with a more accurate temperature control.

The centrifuge method yielded a simple (non-ideal) eutectic phase diagram for the urea–choline chloride system, which shows that it is possible to measure the liquidus phase boundaries of mixtures that are prone to supercooling. One should, however, be careful upon data interpretation for systems that can form co-crystals and/or solid solutions when the samples were prepared from its pure solid constituents.

For the biphenyl–bibenzyl system, no concentration gradient was observed in the liquid phase after centrifugation. However, when measuring other systems, the homogeneity of the liquid phase should be verified again. The liquid composition should be evaluated at different heights for at least one sample on both the hypotectic and hypertectic regions of the phase diagram. It is also recommended to

monitor the temperature of the mixture throughout the whole experiment.

Using the centrifuge method, the solid–liquid equilibrium phase behavior can be determined accurately without the need to recrystallize the mixture from the liquid phase within short time periods. This offers a great advantage when studying the phase behavior of mixtures that exhibit severe supercooling, such as most hydrophilic deep eutectic solvents. The centrifuge method therefore offers a means to rapidly explore the liquid range of eutectic mixtures at the operating temperature of interest and therefore to determine the compositions at which these mixtures can be applied as a liquid.

SUPPLEMENTARY MATERIAL

See supplementary material for more details on the centrifuge overheating, the dependency of DSC peak events on heating rate, and the procedures regarding ^{1}H-NMR analysis. Also presented are the phase behavior data and fitting parameters for the heat capacity, as well as a discussion on the impact of solid solution formation.

ACKNOWLEDGMENTS

Financial support from Netherlands Organization for Scientific Research (NWO) and the company Paques B.V. is gratefully acknowledged. This work is part of the research program "MES meets DES," with Project No. STW–Paques 12999. The technical support provided by Marco M. R. M. Hendrix was highly appreciated. The developers from Avular B.V. are gratefully acknowledged for their dedication to the development and implementation of custom-made temperature loggers that could be used during centrifugation.

[1] A. P. Abbott, G. Capper, D. L. Davies, R. K. Rasheed, and V. Tambyrajah, Chem. Commun. Issue 1, 70 (2003).
[2] J. M. Smith, H. Van Ness, M. Abbott, and M. Swihart, *Introduction to Chemical Engineering Thermodynamics*, 8th ed. (McGraw-Hill Education, New York, 2018).
[3] E. L. Smith, A. P. Abbott, and K. S. Ryder, Chem. Rev. **114**, 11060 (2014).
[4] J. D. Mota-Morales, R. J. Sánchez-Leija, A. Carranza, J. A. Pojman, F. del Monte, and G. Luna-Bárcenas, Prog. Polym. Sci. **78**, 139 (2018).
[5] G. Diarce, L. Quant, Á. Campos-Celador, J. M. Sala, and A. García-Romero, Sol. Energy Mater. Sol. Cells **157**, 894 (2016).
[6] S. N. Gunasekara, V. Martin, and J. N. Chiu, Renewable Sustainable Energy Rev. **73**, 558 (2017).
[7] A. Brodin, A. Nyqvist-Mayer, T. Wadsten, B. Forslund, and F. Broberg, J. Pharm. Sci. **73**, 481 (1984).
[8] C. Leuner and J. Dressman, Eur. J. Pharm. Biopharm. **50**, 47 (2000).
[9] N. R. Rodriguez, T. Gerlach, D. Scheepers, M. C. Kroon, and I. Smirnova, J. Chem. Thermodyn. **104**, 128 (2017).
[10] D. J. G. P. van Osch, L. F. Zubeir, A. van den Bruinhorst, M. A. A. Rocha, and M. C. Kroon, Green Chem. **17**, 4518 (2015).
[11] P. V. A. Pontes, E. A. Crespo, M. A. R. Martins, L. P. Silva, C. M. S. S. Neves, G. J. Maximo, M. D. Hubinger, E. A. C. Batista, S. P. Pinho, J. A. P. Coutinho, G. Sadowski, and C. Held, Fluid Phase Equilib. **448**, 69 (2017).
[12] Y. Dai, G. J. Witkamp, R. Verpoorte, and Y. H. Choi, Food Chem. **187**, 14 (2015).
[13] X. Meng, K. Ballerat-Busserolles, P. Husson, and J.-M. Andanson, New J. Chem. **40**, 4492 (2016).
[14] J. Russo, F. Romano, and H. Tanaka, Phys. Rev. X **8**, 021040 (2018).
[15] L. M. Wang, Z. Li, Z. Chen, Y. Zhao, R. Liu, and Y. Tian, J. Phys. Chem. B **114**, 12080 (2010).
[16] K. Bica, J. Shamshina, W. L. Hough, D. R. MacFarlane, and R. D. Rogers, Chem. Commun. **47**, 2267 (2011).
[17] G. W. H. Höhne, W. F. Hemminger, and H.-J. Flammersheim, *Differential Scanning Calorimetry* (Springer Berlin Heidelberg, Berlin, Heidelberg, 2003).
[18] L. Rycerz, J. Therm. Anal. Calorim. **113**, 231 (2013).
[19] E. B. Ferreira, M. L. Lima, and E. D. Zanotto, J. Am. Ceram. Soc. **93**, 3757 (2010).
[20] A. Jakob, R. Joh, C. Rose, and J. Gmehling, Fluid Phase Equilib. **113**, 117 (1995).
[21] Y. Dai, J. van Spronsen, G.-J. Witkamp, R. Verpoorte, and Y. H. Choi, Anal. Chim. Acta **766**, 61 (2013).
[22] M. Francisco, A. van den Bruinhorst, and M. C. Kroon, Angew. Chem., Int. Ed. **52**, 3074 (2013).
[23] G. Rothenberg, A. P. Downie, C. L. Raston, and J. L. Scott, J. Am. Chem. Soc. **123**, 8701 (2001).
[24] A. I. Kitaigorodsky, in *Mixed Crystals*, edited by M. Cardona (Springer Berlin Heidelberg, Berlin, Heidelberg, 1984), pp. 227–274.
[25] F. M. Acampora, A. S. Tompa, and N. O. Smith, J. Chem. Phys. **24**, 1104 (1956).
[26] C. Suryanarayana, Prog. Mater. Sci. **46**, 1–184 (2001).
[27] R. S. Sokolowski and M. E. Glicksman, J. Cryst. Growth **119**, 126 (1992).
[28] J. F. Löffler, S. Bossuyt, A. Peker, and W. L. Johnson, Appl. Phys. Lett. **81**, 4159 (2002).
[29] L. J. Wittenberg, J. Am. Ceram. Soc. **42**, 209 (1959).
[30] H. A. Friedman, J. Sci. Instrum. **44**, 454 (1967).
[31] R. E. Thoma, H. Insley, H. A. Friedman, and G. M. Hebert, J. Nucl. Mater. **27**, 166 (1968).
[32] J. F. Löffler, S. Bossuyt, A. Peker, and W. L. Johnson, Philos. Mag. **83**, 2797 (2003).
[33] H. H. Lee and J. C. Warner, J. Am. Chem. Soc. **57**, 318 (1935).
[34] H. G. Morrison, C. C. Sun, and S. Neervannan, Int. J. Pharm. **378**, 136 (2009).
[35] J. F. Messerly, H. L. Finke, W. D. Good, and B. E. Gammon, J. Chem. Thermodyn. **20**, 485 (1988).
[36] R. D. Chirico, S. E. Knipmeyer, A. Nguyen, and W. V. Steele, J. Chem. Thermodyn. **21**, 1307 (1989).
[37] D. F. O'Rourke and S. C. Mraw, J. Chem. Thermodyn. **15**, 489 (1983).
[38] G. W. Smith, Mol. Cryst. Liq. Cryst. **49**, 207 (1979).
[39] P. S. Gill, S. R. Sauerbrunn, and M. Reading, J. Therm. Anal. **40**, 931 (1993).
[40] E. A. Crespo, L. P. Silva, M. A. R. Martins, L. Fernandez, J. Ortega, O. Ferreira, G. Sadowski, C. Held, S. P. Pinho, and J. A. P. Coutinho, Ind. Eng. Chem. Res. **56**, 12192 (2017).
[41] V. Steinberg and D. Linsky, Phys. Chem. Liq. **12**, 45 (1982).
[42] K.-S. Kim and B. H. Park, J. Chem. Eng. Jpn. **48**, 881 (2015).
[43] R. L. Collin, J. Am. Chem. Soc. **79**, 6086 (1957).
[44] I. M. Aroso, A. Paiva, R. L. Reis, and A. R. C. Duarte, J. Mol. Liq. **241**, 654 (2017).